Diffraction contrast imaging

Lecture 13

Weak beam dark field imaging

Simulation of diffraction contrast

Weak beam dark field imaging

Weak beam dark field images

Goal: 'high resolution' diffraction contrast image of defects

Method: establish a kinematical condition (large **s**)

This gives a small ξ_{eff}

Result is a narrow dislocation image (since this is proportional to ξ_{eff})

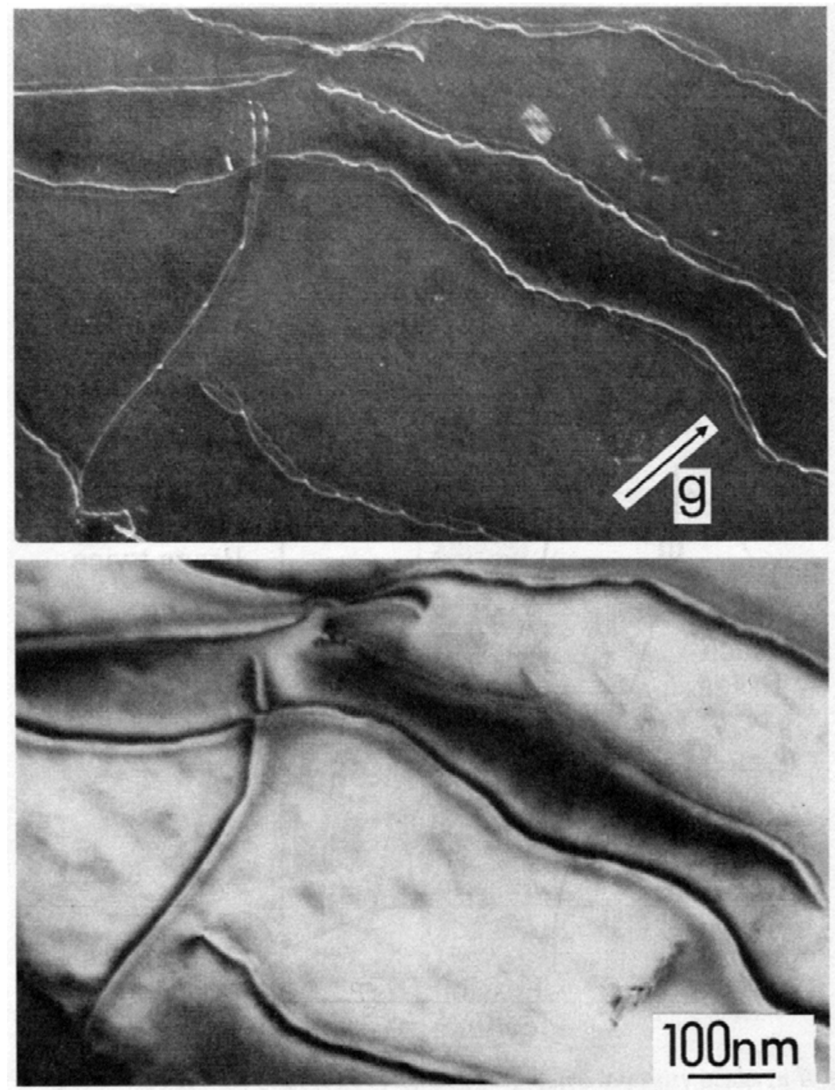

Weak beam dark field images

Why high-resolution images?

Often want to look at:

- Jogs & kinks
- Separation between partial dislocations
- Interaction between dislocations
- Interaction with other defects & precipitates

Again, these images can help correlate specifics of dislocation motion with overall plastic deformation response

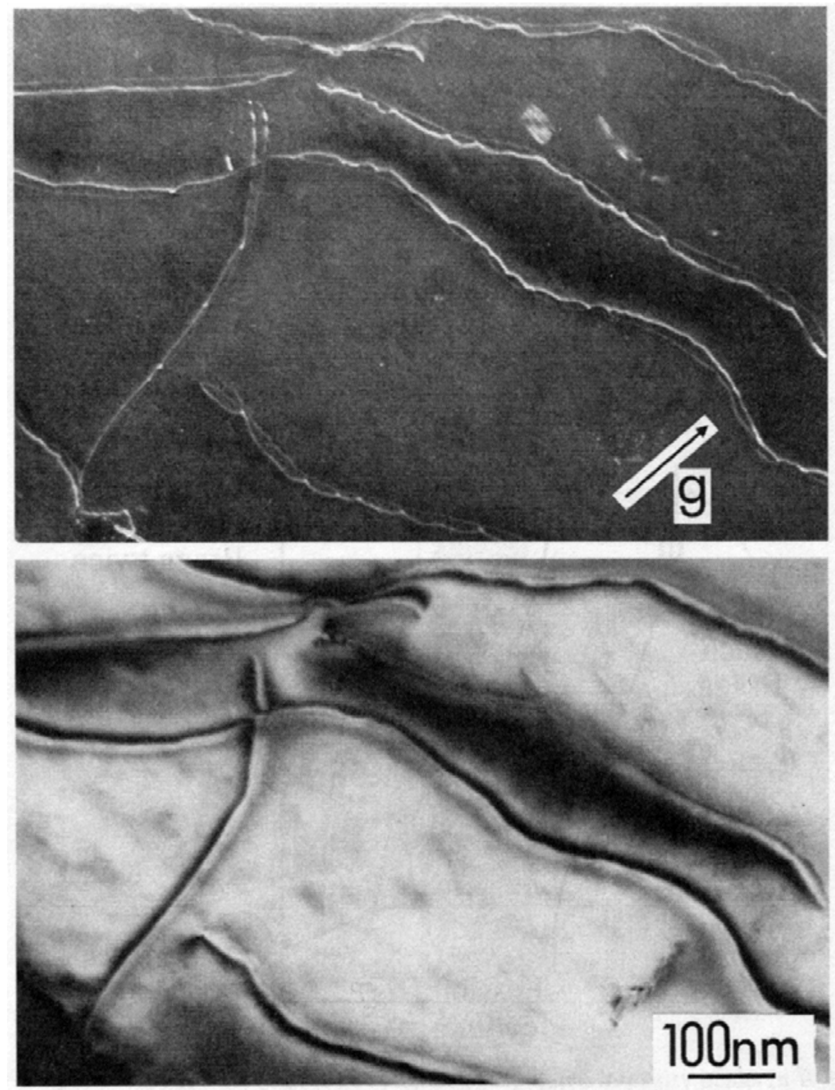

Weak beam dark field imaging

- By setting **s** 'large' most of the sample is <u>not</u> oriented in a strong Bragg condition
- However, defect locally bends planes back to Bragg angle
- The region over which this occurs is very small, as the strain needed must be large
- Thus the defect image is quite narrow
- The image 'peak' is thus close to the dislocation core
  - Will switch with sign of g

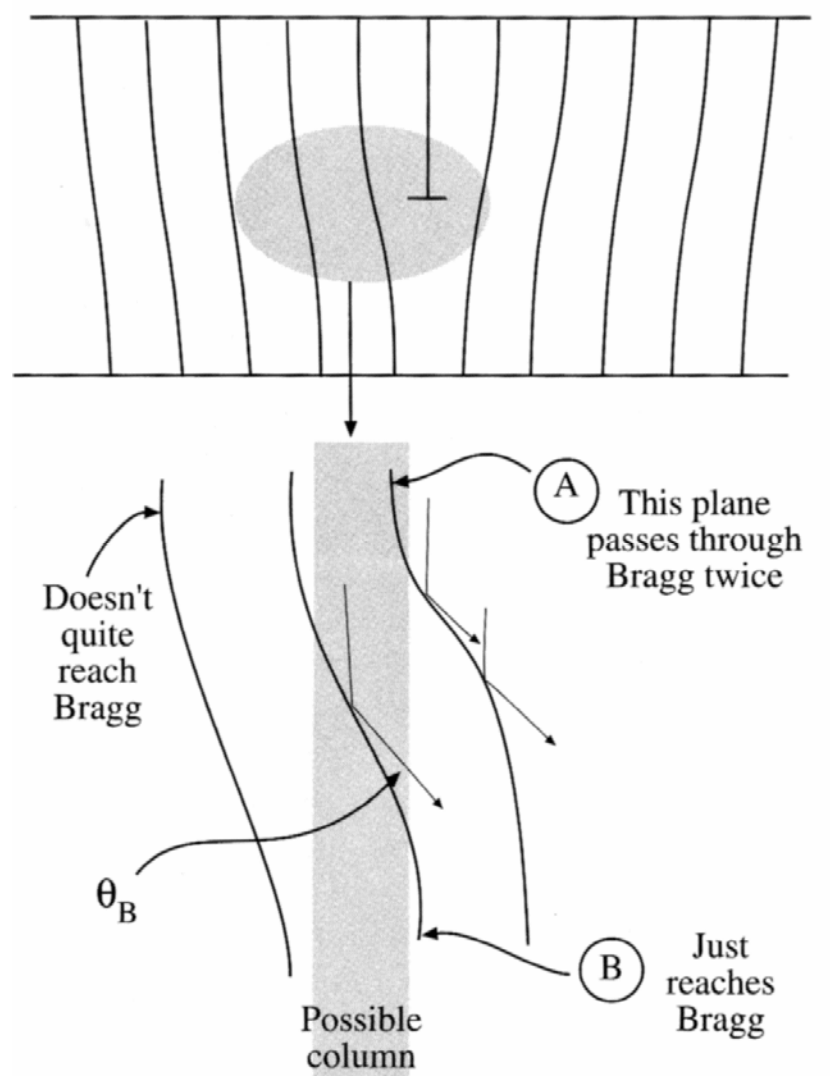

Weak beam dark field imaging

Steps:

1. **Establish two beam condition with s slightly greater than zero**
2. **Tilt the strong g to the optic axis using dark field tilts**
   - You will note that it becomes quite dim
   - You will also see 3g become strong
     - This is purely a geometric effect
3. **Insert objective aperture & check centering**
4. **Now both BF & WBDF are well established**

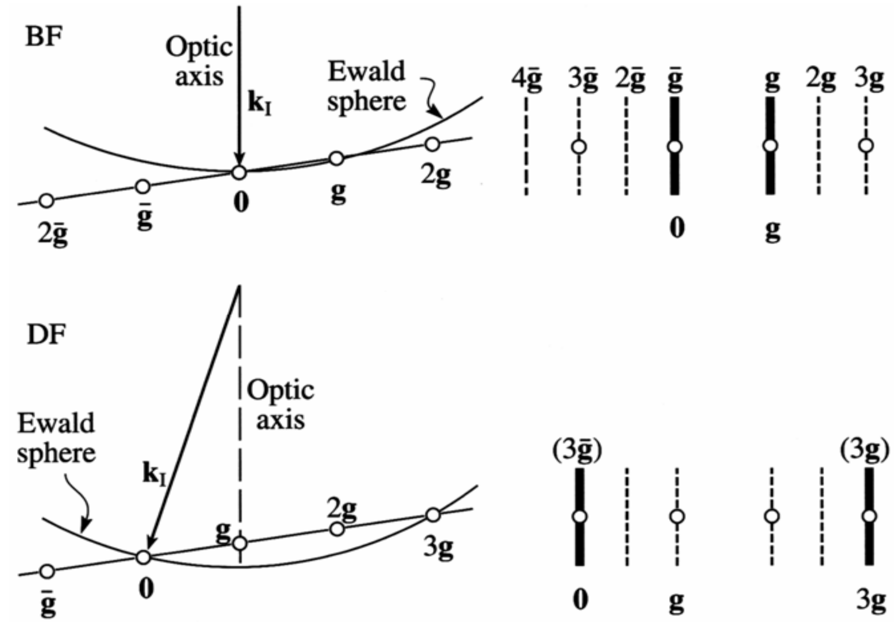

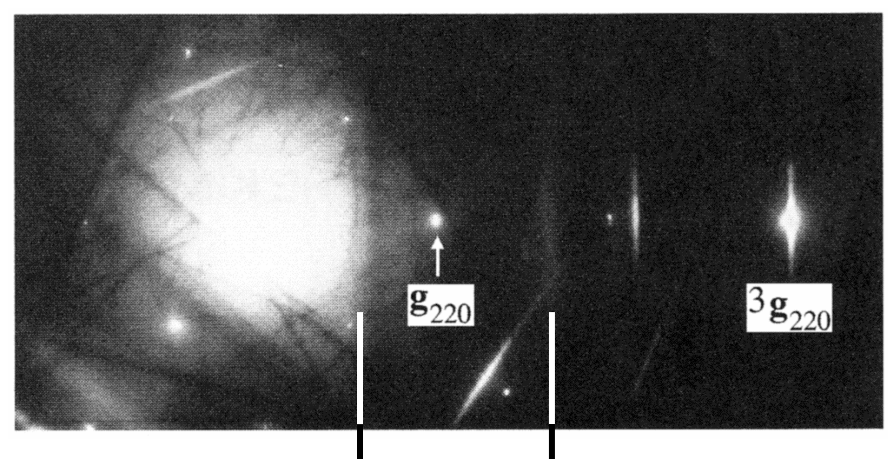

Weak beam dark field imaging

- Nothing ‘magical’ about the g-3g condition
  - It’s just one that ‘often’ works
- Any two-beam condition where corresponding DF has s >> 0 will work, and some may work better
- For calculation purposes, may need to know s precisely
  - Measurement method described in W&C text
- Resulting WBDF image will have ‘weak’ intensity
  - May require very long exposures
  - Resolution limit may be stage drift

Weak beam dark field imaging

A bit of theory

$$I_g = |\phi_g|^2 = \left(\frac{\pi t}{\xi_g}\right)^2 \frac{\sin^2(\pi s_{eff} t)}{(\pi s_{eff})^2} \qquad s_{eff} = \sqrt{s^2 + \frac{1}{\xi_g^{\ 2}}}$$

If $s \gg 0$, then $s_{eff} \approx s$

Resulting image largely insensitive to ξ_{eff}

Image is 'kinematical'

$$I \propto \frac{\sin^2(\pi s_z t)}{(\pi s_z)^2}$$

Weak beam dark field imaging

So - in most of the image - we have kinematical contrast

- $\vec{0}$ and $\vec{g}$ are not strongly coupled

However - local to the defect - the two beams are strongly coupled

- The defect is the connecting link
- Strong dynamical contrast only local to the defect

Bloch wave explanation:

- Defect causes local change in scattering from Bloch Wave #1 to Bloch Wave #2

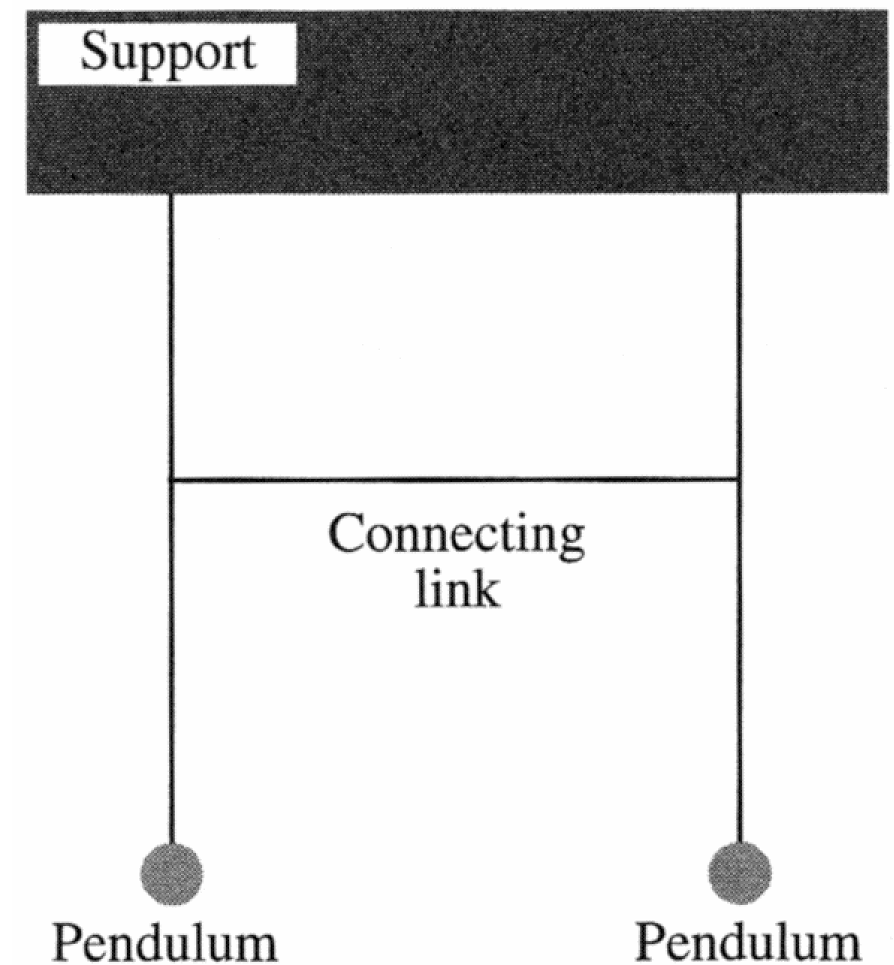

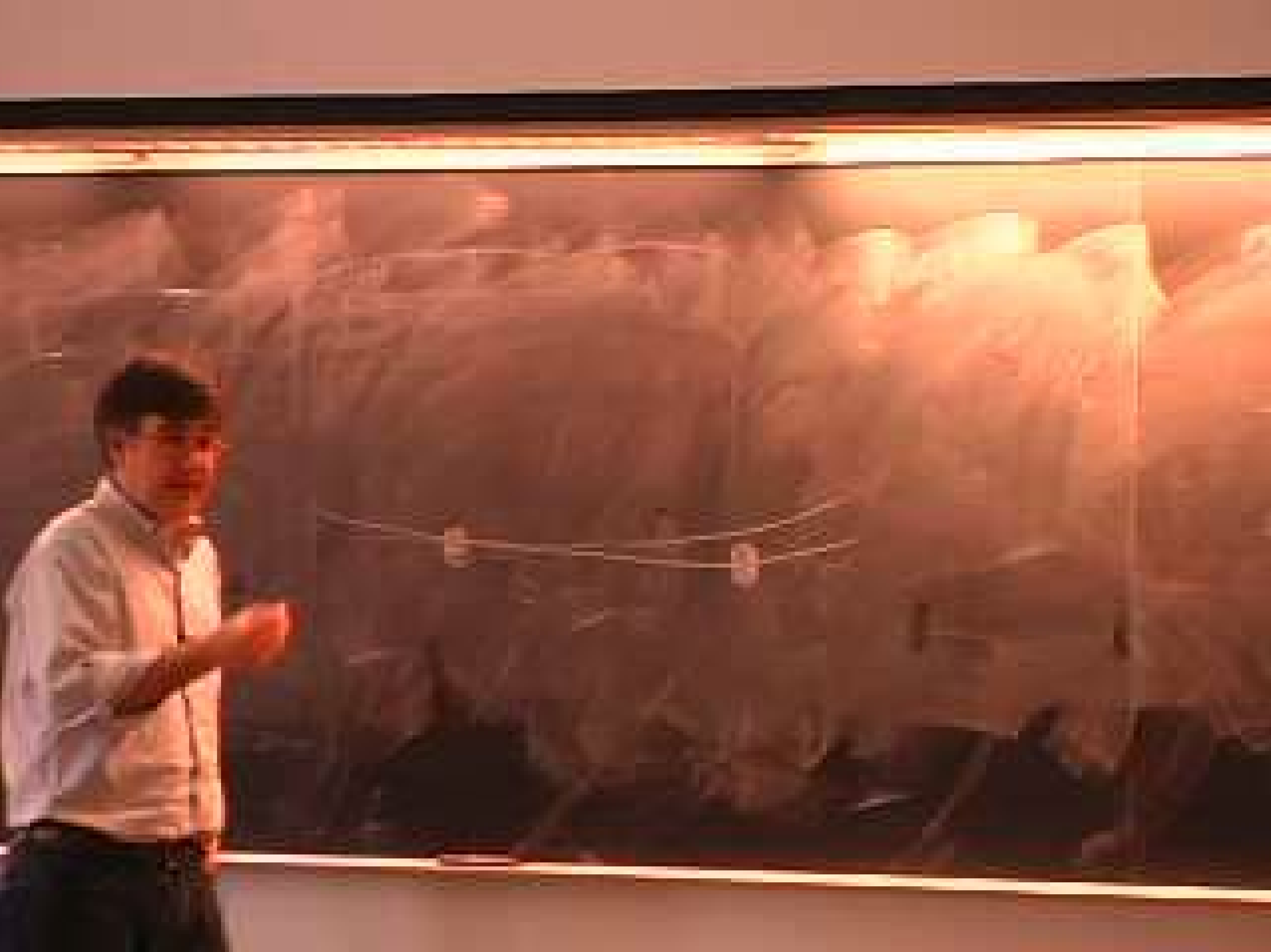

Weak beam dark field imaging

So - in most of the image - we have kinematical contrast

- $\vec{0}$ and $\vec{g}$ are not strongly coupled

However - local to the defect - the two beams are strongly coupled

- The defect is the connecting link
- Strong dynamical contrast only local to the defect

Bloch wave explanation:

- Defect causes local change in scattering from Bloch Wave #1 to Bloch Wave #2

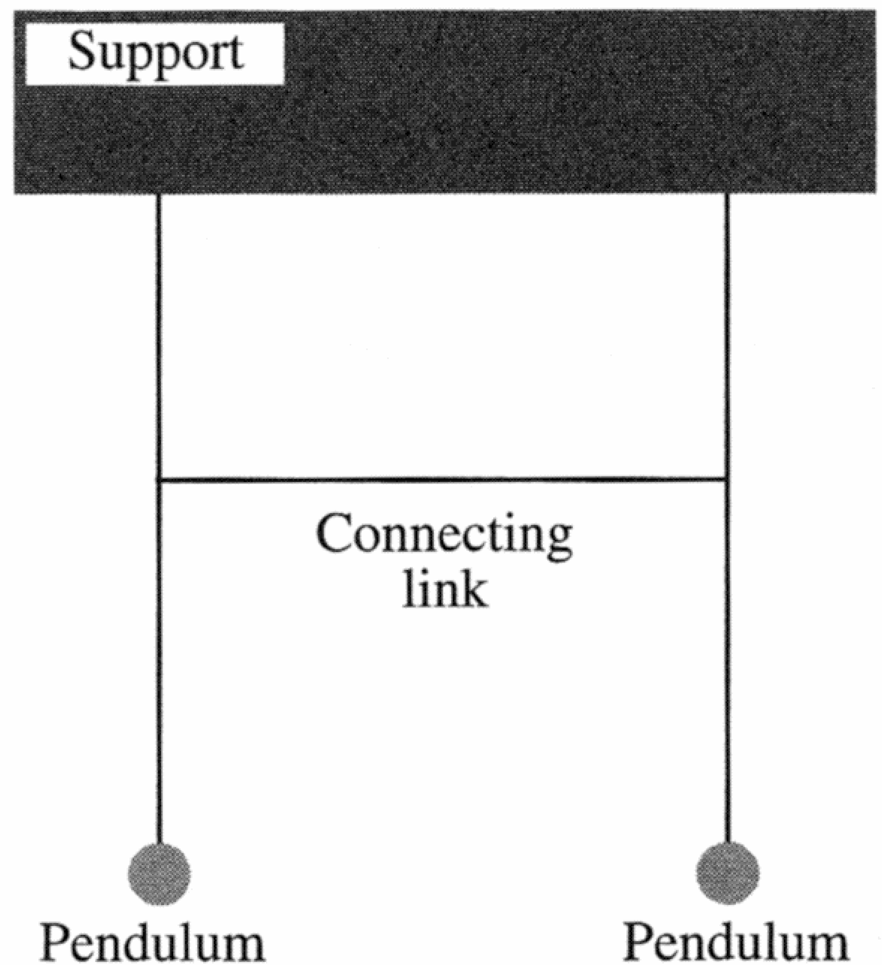

Weak beam dark field imaging

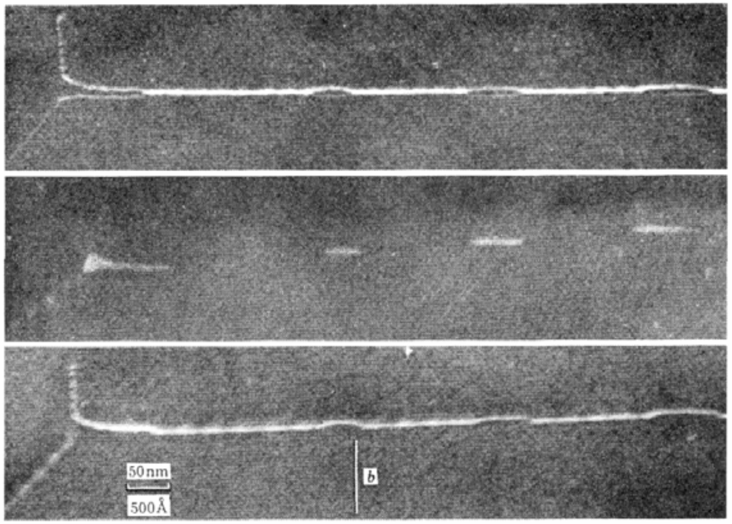

Can more readily see dissociation & interaction effects

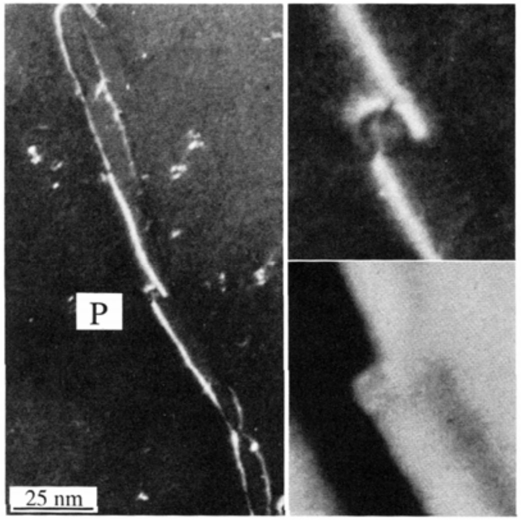

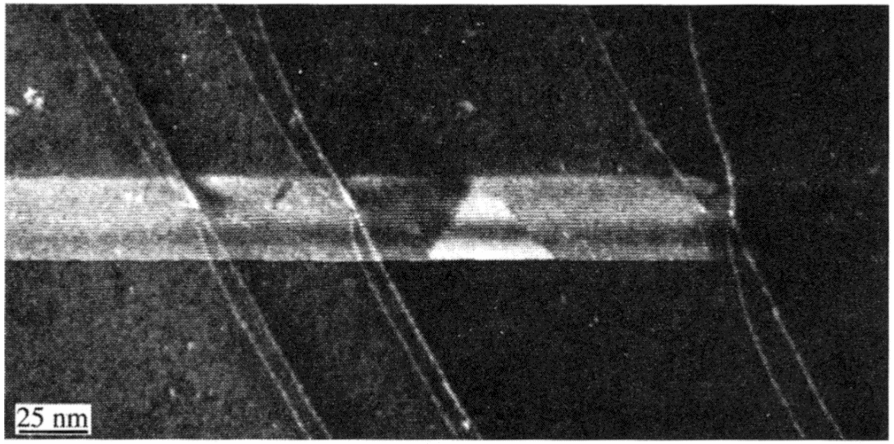

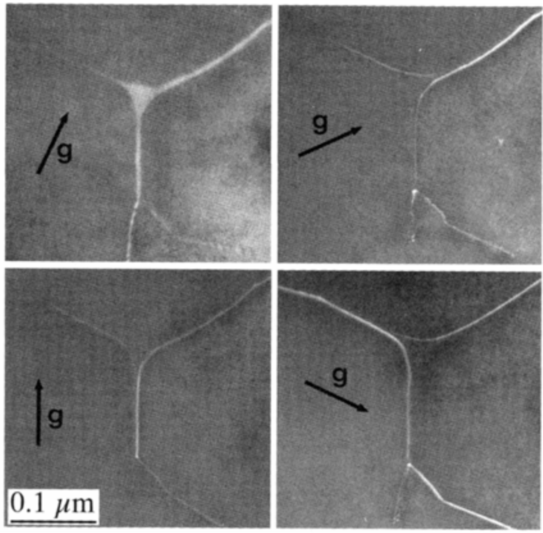

Weak beam dark field imaging

Inside-outside contrast also sensitive to small changes in s during WBDF imaging

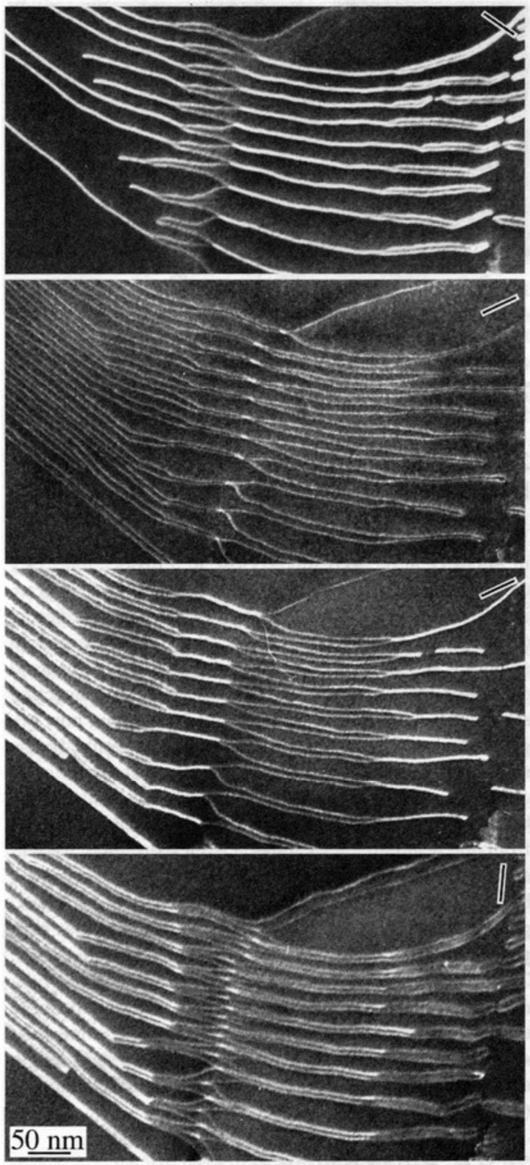

Weak beam dark field imaging

Many more fringes seen in SF images

Spacing very sensitive to s

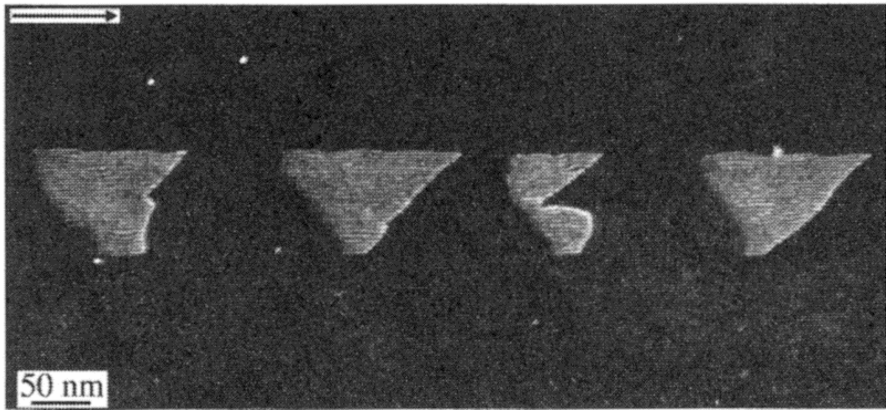

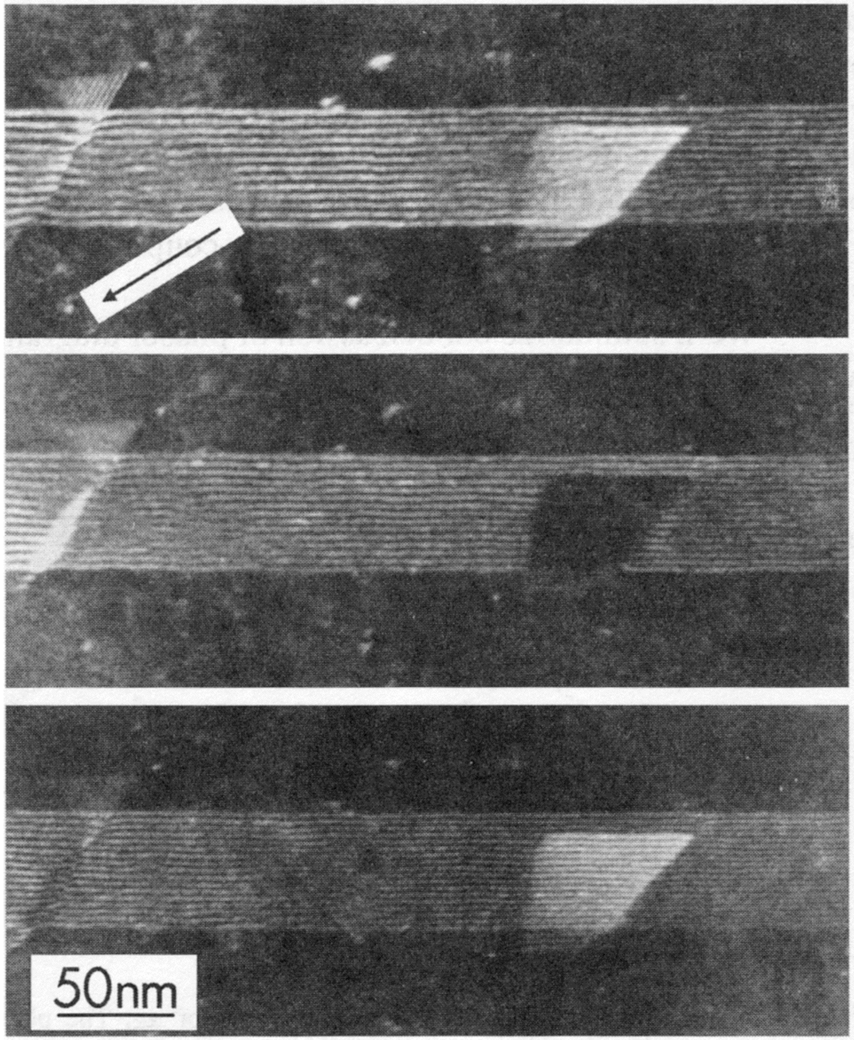

Weak beam dark field imaging

Strong effect on thickness fringe spacing as well

Large **s** reduces effective extinction distance ξ_{eff}

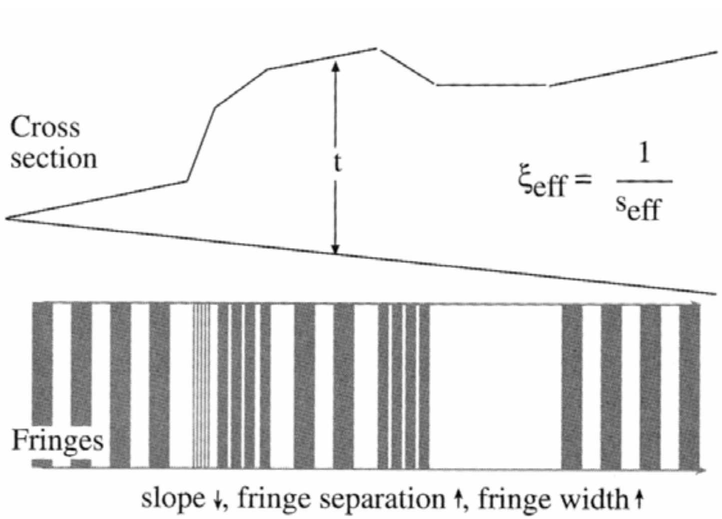

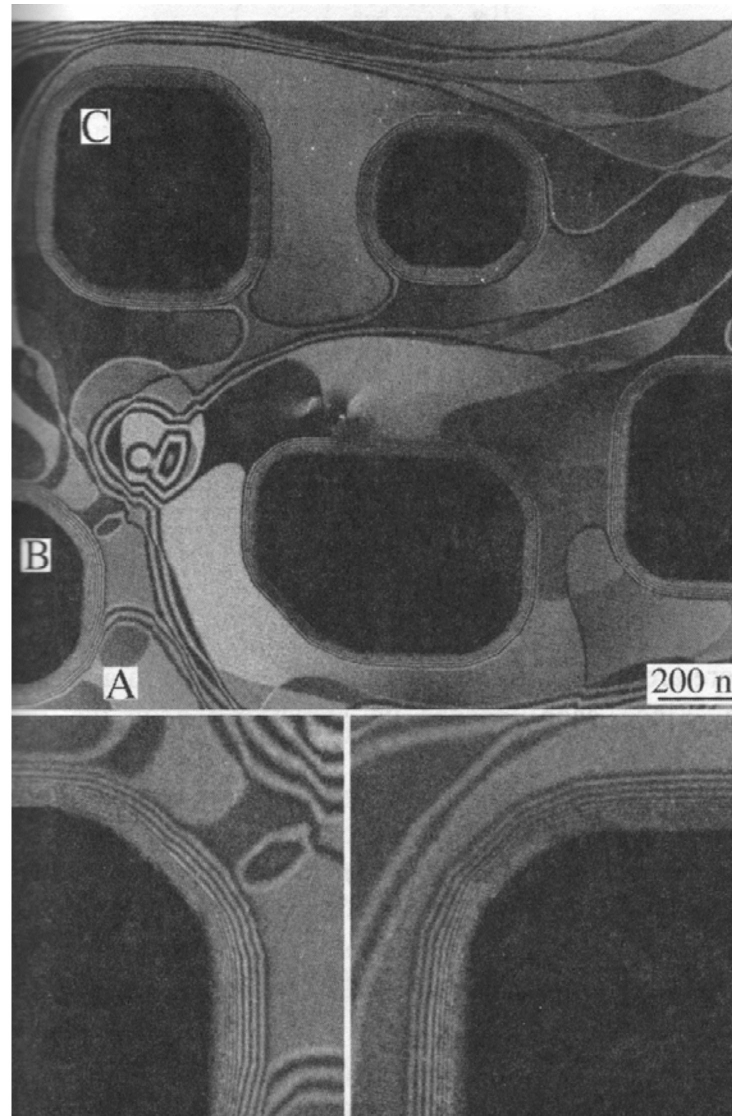

Simulation of diffraction contrast

Computational solutions to HW Eqns

Use:

$$\frac{d\phi_g}{dz} = \frac{\pi i}{\xi_g}\phi_o \exp\left[-2\pi i\left(sz + \vec{g}\cdot\vec{R}\right)\right] + \frac{\pi i}{\xi_o}\phi_g$$

and

$$\frac{d\phi_o}{dz} = \frac{\pi i}{\xi_g}\phi_o + \frac{\pi i}{\xi_o}\phi_g \exp\left[2\pi i\left(sz + \vec{g}\cdot\vec{R}\right)\right]$$

or:

$$\frac{d\phi_o}{dz} = \frac{\pi i}{\xi_o}\phi_g$$

and

$$\frac{d\phi_g}{dz} = \frac{\pi i}{\xi_g}\phi_o + \left[2\pi i\left(sz + \vec{g}\cdot\frac{d\vec{R}}{dz}\right)\right]\phi_g$$

Computational solutions to HW Eqns

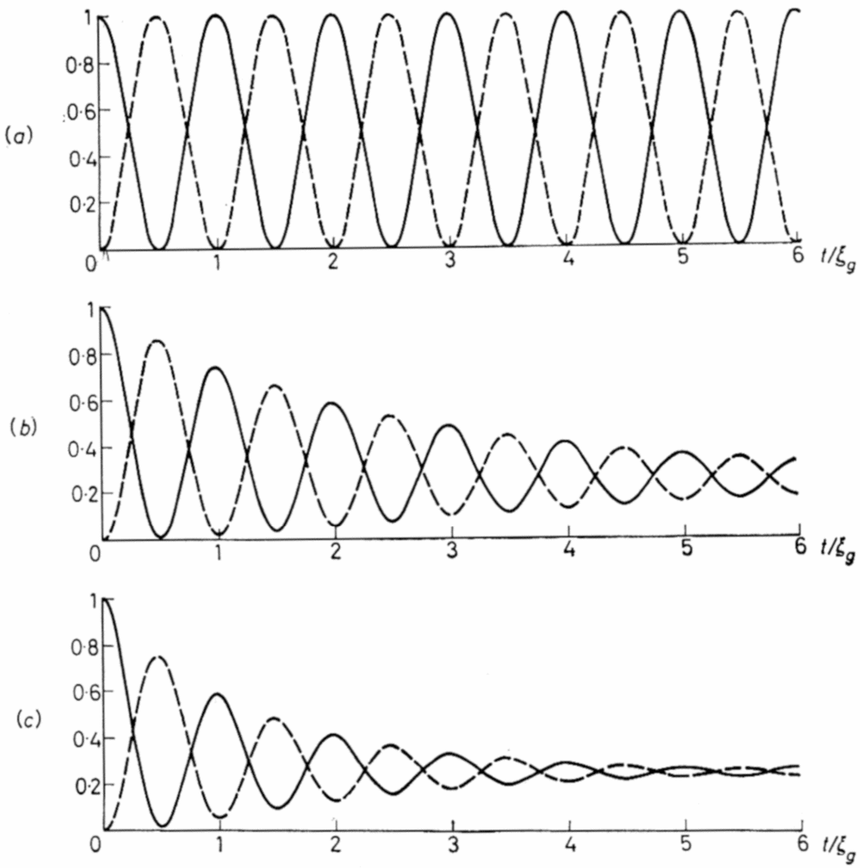

Figure 8.4. Theoretical profiles of thickness fringes. (a) No absorption. (b) $\xi_g/\xi_g' = 0{\cdot}05$. (c) $\xi_g/\xi_g' = 0{\cdot}10$. Note the reduced visibility of the fringes in the thick regions of (c). Continuous and broken lines refer to bright-field and dark-field images respectively
(From Hashimoto, Howie and Whelan, 1962, by courtesy of The Royal Society)

Thickness fringes

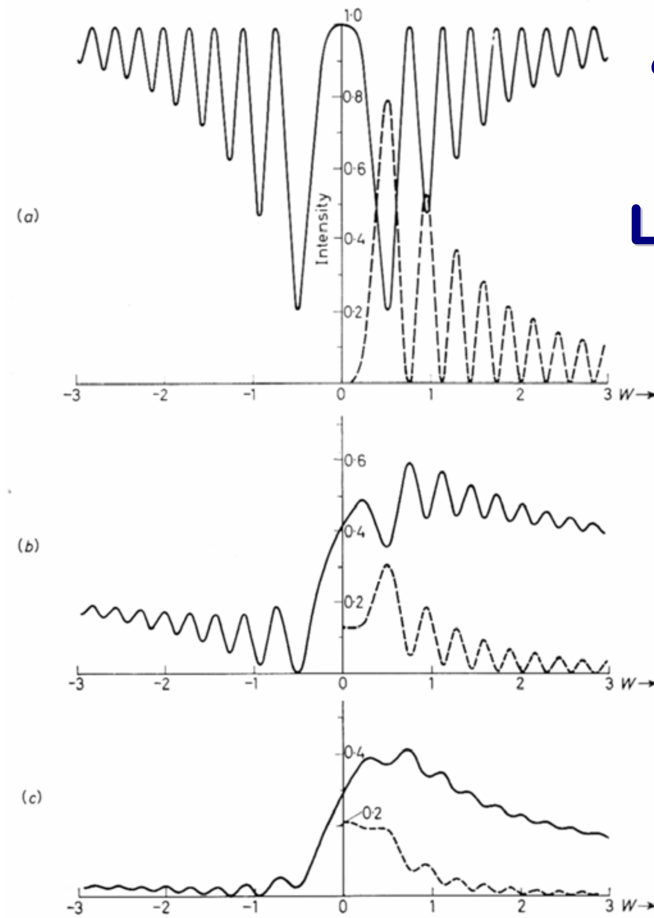

Figure 8.5. 'Rocking Curves' computed on the two-beam theory for a crystal of thickness $t = 4\xi_g$. Full curves are bright-field images; broken curves are dark-field images. The dark-field images are symmetrical about $w = s\xi_g = 0$. (a) No absorption, $\xi_g/\xi_g' = 0$. (b) $\xi_g/\xi_g' = 0{\cdot}05$. (c) $\xi_g/\xi_g' = 0{\cdot}10$. The curves in (a) are complementary. Note the asymmetry of the bright-field images in (b) and (c) (corresponding to either edge of the dark band at D in Figure 8.3), and the reduced amplitude of the subsidiary oscillations in (c). In (b) and (c) $\xi_0' = \xi_g'$
(From Hashimoto, Howie and Whelan, 1962, by courtesy of The Royal Society)

"Rocking" Curve

Like a trace across a bend contour

$$\mathbf{w} = \mathbf{s}\xi_{\mathbf{g}}$$

Computational solutions to HW Eqns

Obviously, can produce simulated images by calculating ϕ_o and ϕ_g along each column

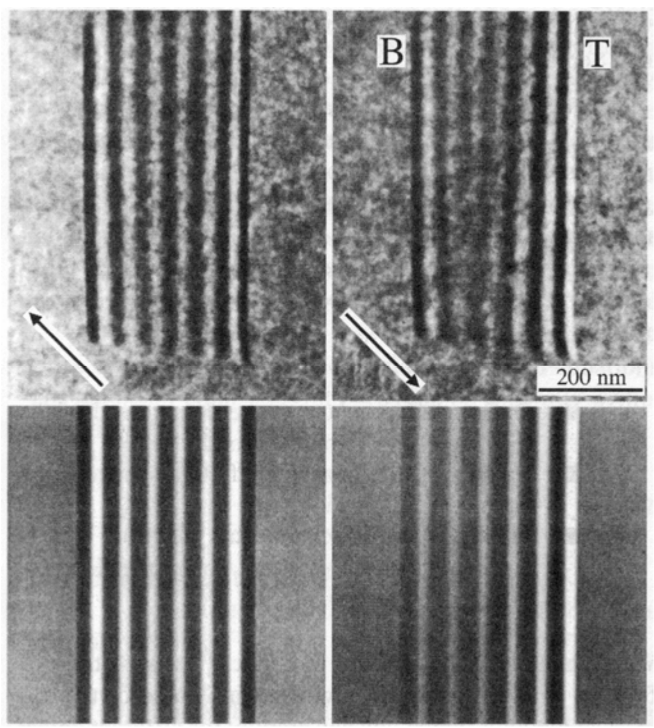

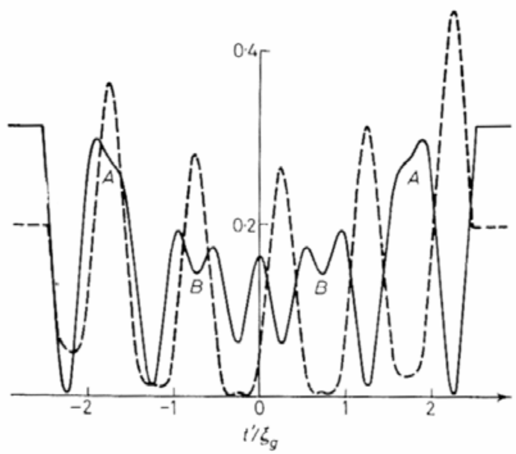

Figure 10.9. Computed stacking fault image profile for $\alpha = -2\pi/3$ with anomalous absorption effects included, $t/\xi_g = 5$, $\xi_0' = \xi_g'$, $\xi_g/\xi_g' = 0{\cdot}07$, $w = 0$. Bright- and dark-field images are shown as continuous and broken lines respectively
(From Hashimoto, Howie and Whelan, 1960, by courtesy of *The Philosophical Magazine*)

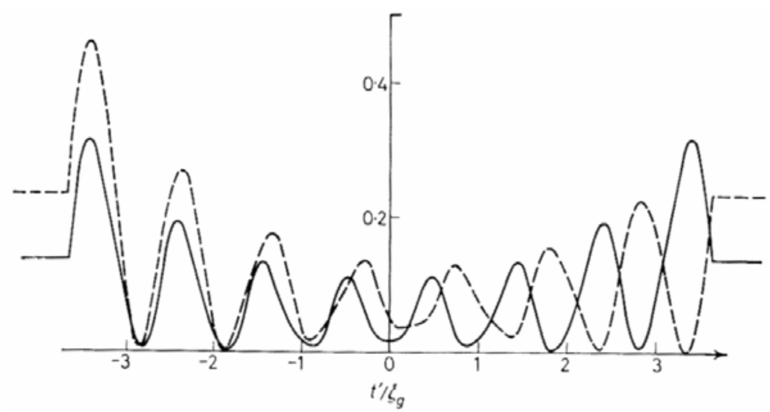

Figure 10.8. Computed stacking fault image profile for $\alpha = +2\pi/3$ with anomalous absorption effects included, $t/\xi_g = 7{\cdot}25$, $\xi_0' = \xi_g'$, $\xi_g/\xi_g' = 0{\cdot}075$, $w = -0{\cdot}2$. Bright- and dark-field images are shown as continuous and broken lines respectively
(From Hashimoto, Howie and Whelan, 1962, by courtesy of The Royal Society)

Computational solutions to HW Eqns

Dislocations show relatively sharp fall-offs in contrast

Due to the nature of $\dfrac{dR}{dz}$

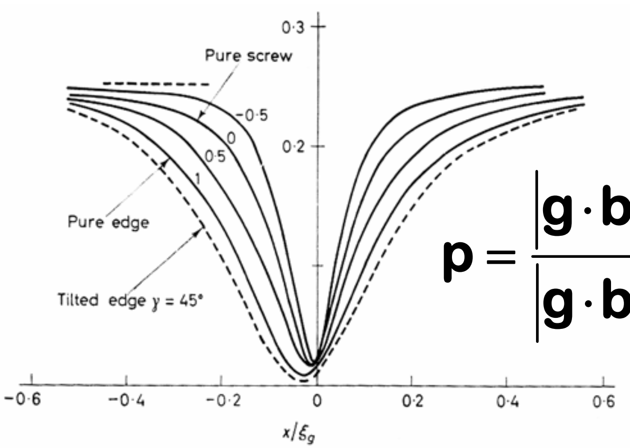

$$p = \frac{|g \cdot b_e|}{|g \cdot b_s|}$$

Figure 11.11. Computed bright-field images of mixed dislocations. The image width depends on the value of the parameter p shown for each curve. See text for discussion
(From Howie and Whelan, 1962, by courtesy of The Royal Society)

Partial

Screw

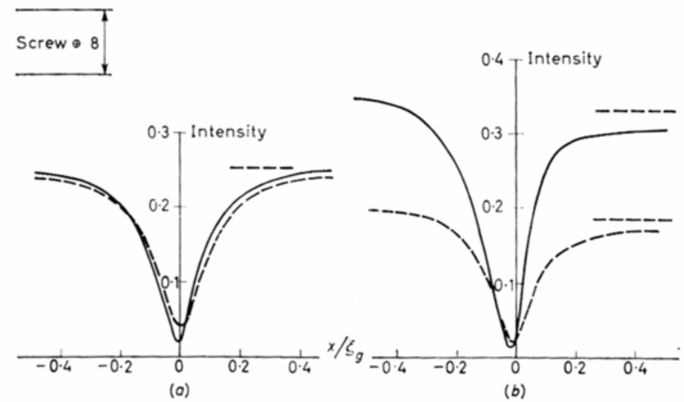

Figure 11.4. Computed bright-field (continuous line) and dark-field (broken line) images for a screw dislocation in the middle of a thick foil with $t = 8\xi_g$, $\mathbf{g.b} = 1$, $\xi_g/\xi_g' = 0{\cdot}1$. *In (a)* $w = 0$; *in (b)* $w = 0{\cdot}3$
(From Howie and Whelan, 1962, by courtesy of The Royal Society)

Edge

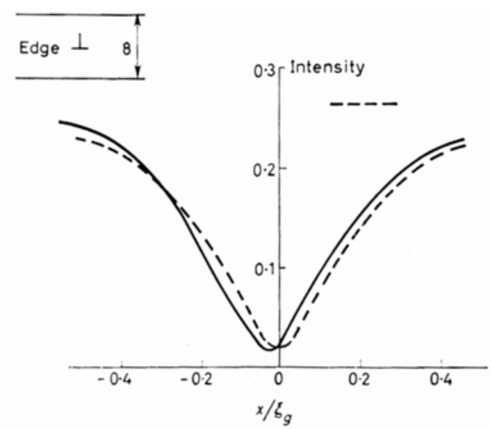

Figure 11.5. Computed bright- and dark-field images for an edge dislocation in the middle of a thick foil with $t = 8\xi_g$, $\mathbf{g.b} = 1$, $\xi_g/\xi_g' = 0{\cdot}1$, $w = 0$. *Compare with Figure 11.4a*

Computational solutions to HW Eqns

"A method for simulating electron microscope dislocation images," *Schublin R., Stadalmann P.,* Materials Science and Engineering, A 164 (1993) 378-378

Computed Electron Micrographs and Defect Identification, *Head A.K., Humble P., Clarebrough L.M., Morton A.J.* and *Forwood C.T.,* North-Holland Publishing Company, Amsterdam, 1973

CUFOUR:

-http://cecm.insa-lyon.fr/CIOL/cufour.html

Computational solutions to HW Eqns

Obviously, can produce simulated images by calculating ϕ_o and ϕ_g along each column

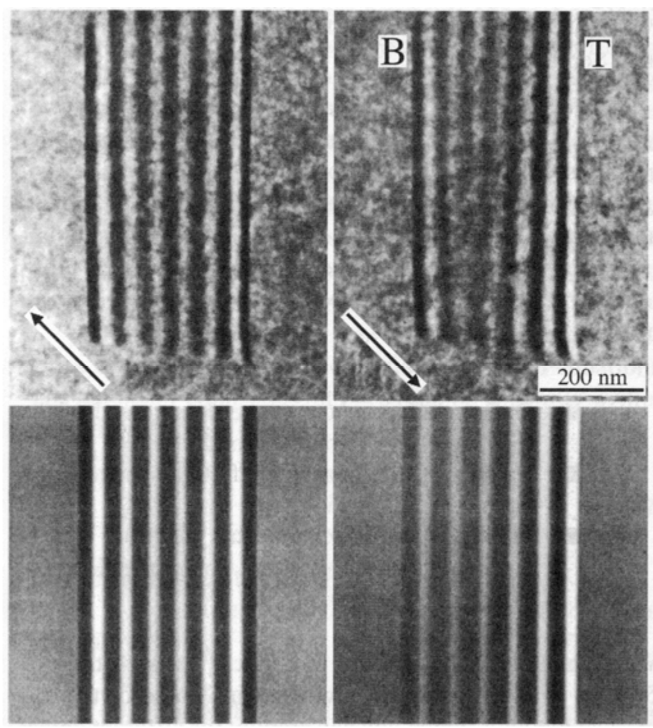

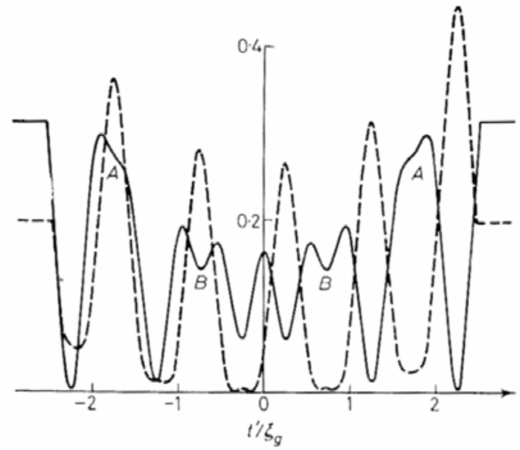

Figure 10.9. Computed stacking fault image profile for $\alpha = -2\pi/3$ with anomalous absorption effects included, $t/\xi_g = 5$, $\xi_0' = \xi_g'$, $\xi_g/\xi_g' = 0{\cdot}07$, $w = 0$. Bright- and dark-field images are shown as continuous and broken lines respectively
(From Hashimoto, Howie and Whelan, 1960, by courtesy of *The Philosophical Magazine*)

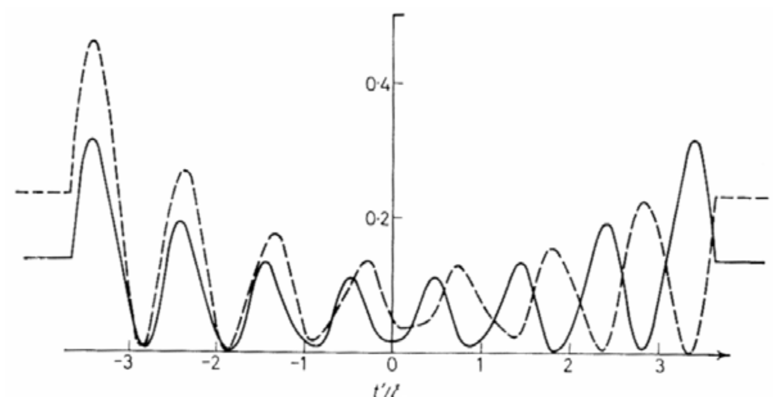

Figure 10.8. Computed stacking fault image profile for $\alpha = +2\pi/3$ with anomalous absorption effects included, $t/\xi_g = 7{\cdot}25$, $\xi_o' = \xi_g'$, $\xi_g/\xi_g' = 0{\cdot}075$, $w = -0{\cdot}2$. Bright- and dark-field images are shown as continuous and broken lines respectively
(From Hashimoto, Howie and Whelan, 1962, by courtesy of The Royal Society)

Computational solutions to HW Eqns

"SIMCON" ▪

A program that allows one to use the output form FEM modeling to generate simulated diffraction contrast

K. Janssens, Ultramicroscopy, 45, 323, 1992.

J. Demarest, et al., Appl. Phys. Lett., 77, 412, 2000.

Li, et al., Appl. Phys. Lett. 87, 222111, 2005.

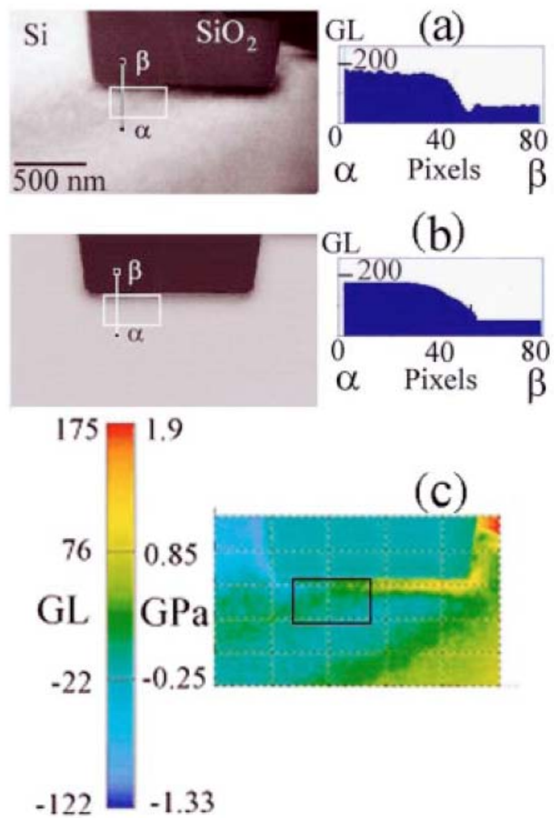

FIG. 1. (Color) Experimental (400) TEM image of shallow isolation trench structure and line scan (a). Simulated (400) TEM image of shallow isolation trench structure and line scan (b). Difference map created by subtracting a from b on a pixel by pixel basis (c). Boxes show the analyzed regions.

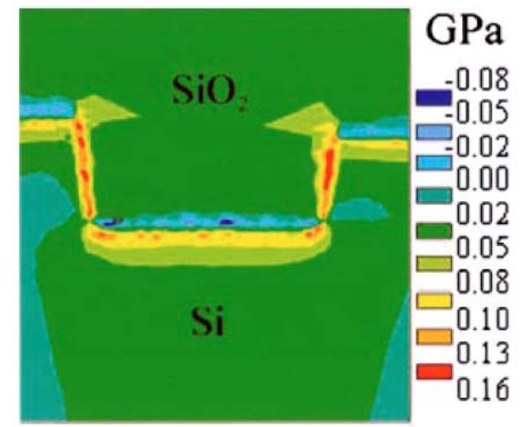

FIG. 3. (Color) ANSYS stress plot of y-axis stresses (vertical in the plane of the page) surrounding the shallow isolation trench structure. Note: entire FE model not shown.